

# Sintering study of calcium aluminate

V. K. SINGH

*Department of Ceramic Engineering, Institute of Technology, Banaras Hindu University, Varanasi-221005, India*

Measurement of the initial sintering shrinkage of  $\text{CaAl}_2\text{O}_4$  at temperatures of 1300, 1325 and 1350 °C are reported. The particle sizes chosen were  $-53 + 45$ ,  $-63 + 53$  and  $-75 + 63$  microns and the soaking periods were from 15 to 360 min. A time dependence of the shrinkage has shown that volume diffusion is the dominant mechanism of sintering. At any given time and temperature, the per cent shrinkage was found to be a decreasing function of particle size. The activation energy for the sintering of  $\text{CaAl}_2\text{O}_4$  was found to be  $766.38 \text{ KJ mol}^{-1}$ .

## 1. Introduction

Calcium aluminates are important constituents of high alumina cement and refractory castables. They can be used for constructing flame detectors, for the inner walls of concrete pressure vessels serving as the radiation shield of nuclear reactors and for aircraft landing pads. A mix of calcium aluminate and fused silica aggregate is useful in casting rocket nozzles and a similar mix has been tested for infilling the stainless steel honeycomb acting as protection to missiles during atmospheric re-entry. Calcium aluminates offer a very good host lattice which can be doped with suitable ions to develop solid state lasers and high temperature ceramic sensors after proper densification. A literature survey reveals that very little work has been done towards understanding their sintering behaviour during firing. The present investigation has been conducted in order to study the sintering characteristics of  $\text{CaAl}_2\text{O}_4$  with a view to developing dense polycrystalline calcium aluminate ceramics.

Good mechanical properties in pressed powder compacts are achieved by means of heat treatments. Particles which touch each other in the green state and are the only points of contact become closer and mass transfer takes place along the contact area. The surface curvature of particles varies from point to point within a powder compact and thus the chemical potential of atoms or ions may vary with their position. At higher temperatures, the chemical potential gradients produce the diffusional fluxes necessary for material transport. The rate at which the process can take place is limited by the diffusion coefficient [1]. Material transport from the region between particle centres causes the centres to move towards each other. If the centres of all the particles in the powder compact approach each other, gross shrinkage in sample occurs. The initial sintering shrinkage of a powder compact resulting from the formation of necks between the powder particles through diffusion is represented by

the relationship [1–5]

$$\frac{\Delta L}{L_0} = \left( \frac{Ka^3D}{kTr^p} \right)_{m_t} t^m \quad (1)$$

where  $\Delta L/L_0$  is the fractional shrinkage after time  $t$  at temperature  $T$ ,  $\gamma$  is the surface energy of solid,  $a^3$  is the volume which is directly proportional to the molecular volume of the solid,  $r$  is the particle radius,  $D$  is the diffusivity of the mobile species,  $k$  is the Boltzmann constant and  $K$ ,  $m$  and  $p$  are numerical constants. If it is assumed that both the surface energy  $\gamma$  and particle radius  $r$  are independent of temperature then, if a given powder compact is sintered at constant temperature, the quantities in the bracket on the right hand side of Equation 1 should remain constant so that the equation assumes the simplified form

$$\frac{\Delta L}{L_0} = At^m \quad (2)$$

The value of the power  $m$  has been predicted using models having various degrees of sophistication, but there is general agreement that it should have a value in the range of 0.40–0.50 for volume diffusion and in the range 0.31–0.33 for pure grain boundary diffusion [1, 2, 6]. It has also been reported [4] that the apparent value of the power  $m$  may vary if more than one transport mechanism operate simultaneously. In such an event it is likely that the relative contribution of the different mechanisms and hence the observed value of  $m$  will vary with temperature. No such variation was observed in the sintering of  $\text{CaAl}_2\text{O}_4$  in the temperature range investigated in the present experiments.

The theoretical models assume that a compact of smooth-surfaced particles in point contact is brought instantaneously to sintering temperature at time  $t = 0$  and, as such ideal conditions cannot be met in practice, it is usual to apply time and shrinkage corrections to the measured data. It should be noted, however, that the correction might be needed even if it were

possible to bring the compact instantaneously to a uniform sintering temperature, since a compact of real powder is unlikely to initially behave like the idealized model for which the theory is derived. If the shrinkage data is to be analysed to determine the temperature dependence of sintering rate then, if it is assumed that both the surface energy  $\gamma$  and the particle radius  $r$  are constant, the Equation 1 may be transformed into

$$\frac{\Delta L}{L_0} = \left( \frac{K'D}{T} \right)^m t^m$$

so that

$$\log K'D = (1/m) \log(\Delta L/L_0) - \log t + \log T \quad (3)$$

where  $K'$  is a new constant which is independent of temperature. Thus the activation energy  $Q$  can be obtained by plotting  $\log(K'D)$  as a function of  $1/T$ , where  $\Delta L/L_0$  and  $t$  may be determined at a given temperature from any point chosen on the shrinkage plot. In a sintering experiment the shrinkage is measured as a function of time; therefore, the data yields a sintering rate at different values of shrinkage, making it possible to obtain Arrhenius plots at a fixed value of shrinkage. In order to make the data more meaningful, the activation energy has been determined at a 3.0% volume shrinkage at different temperatures for  $-75 + 63$ ,  $-63 + 53$  and  $-53 + 45$  micron powder compacts of mono-calcium aluminate.

## 2. Experimental procedure

Monocalcium aluminate was prepared by heating a 1:1 molar mix of analytical reagent quality calcium carbonate and aluminium oxide at  $1350^\circ\text{C}$  for 2 h. The fired material was powdered to  $-75$  micron size and refired at  $1350^\circ\text{C}$  for 2 h so that the reactants and reaction intermediates had completely disappeared [7]. The phase analysis [8] was done by X-ray diffraction study (JCPDS: 23-1036). The CA ( $\text{C} = \text{CaO}$ ,  $\text{A} = \text{Al}_2\text{O}_3$ ) so obtained was ground to  $-75$  micron fineness in an agate ball mill and graded as  $-75 + 63$ ,  $-63 + 53$ ,  $-53 + 45$  and  $-45$  micron powders.

The true density of the material was  $2.98 \text{ g cm}^{-3}$ . The effect of forming pressure was studied by pressing the  $-45$  micron powders at 75, 150, 225, 300, 375 and 450 MPa. For the measurement of initial sintering shrinkage, samples having different particle sizes were pressed separately under a hydraulic press at 150 MPa in the form of pellets of 12.5 mm diameter using a steel die. Pellets were compacted with a small addition of rectified spirit under a constant rate of loading and held for 30 s at 150 MPa. They were prefired at  $900^\circ\text{C}$  for 10 min and their bulk volume was determined by the mercury displacement method. Sintering was performed in a two zone silicon carbide resistance heating furnace at 1300, 1325 and  $1350^\circ\text{C}$  for 10–360 min. Prefired samples kept in platinum dishes were placed in the preheating zone of the furnace maintained at  $900^\circ\text{C}$  and were kept at this temperature for 10 min. Preheated pellets were then pushed into the sintering

zone maintained at the set sintering temperature and kept there for the desired sintering time. A Pt–13% Rh–Pt thermocouple tip was placed close to the pellets in the sintering zone of the furnace. The thermocouple emf was measured with the help of a potentiometer. After the desired sintering time pellets were taken back into the preheating zone and kept there for 10 min. Samples were taken out of the furnace and stored in a desiccator. The volume of pellet after firing was again determined by means of a mercury densitometer.

## 3. Results

### 3.1. Evaluation of the power $m$

Pressed powder pellets exhibit an irreversible expansion [3, 9] because of the release of elastic strain within the powder particles when first heated to a temperature just below that required to produce sintering shrinkage. The strain is locked into the pressed particles at room temperature which requires a substantial temperature increase before it can be released. If it is desired to obtain shrinkage measurements of sufficient quality to justify comparison with predictions derived from theoretical models of the sintering process, it is necessary to measure the initial dimensions of the powder compacts after the initial expansion has been triggered. The change in initial dimensions is relatively insignificant because specimen shrinkage can arise only because of the growth of established necks between the particles. Any error in the measurement of initial volume could be expected to cause substantial variations in the measured value of  $m$ . By plotting and replotting the model data, it has been shown [3] that a 0.5% error in the assumed initial volume could cause the apparent value of  $m$  to be reduced from 0.45 to 0.37. In the present work a reproducible value of  $m$  was obtained by prefiring the samples at  $900^\circ\text{C}$  for 10 min. Some of the calcium aluminate pellets showed a lack of reproducibility in the initial expansion during prefiring but it was found that greatly improved reproducibility could be obtained by drying the pressed pellets at  $110^\circ\text{C}$  overnight in an air oven before heating them to  $900^\circ\text{C}$ .

Since the pellets had been formed by uniaxial pressing in a steel die, the dilation was expected to be anisotropic. It was observed that pellets pressed at different pressures exhibited approximately the same difference in percentage dilation between the axial and diametrical dimensions. This indicates that the extent to which the dilation was anisotropic was insensitive to forming pressure. Fig. 1 shows the sintering shrinkage of  $-45$  micron particle size CA powder compacts pressed at 75, 150, 225, 300, 375, 450 MPa and fired at  $1300^\circ\text{C}$  for 1 h after prefiring. The per cent dilation on prefiring along the diameter was almost the same as that obtained in the thickness measurements by a screw gauge. Hence an average effective pressure of 150 MPa was chosen for pressing the  $-75 + 63$ ,  $-63 + 53$  and  $-53 + 45$  micron CA powders which is expected to produce point contacts in the compact. The sintering shrinkage was measured as a volume shrinkage by mercury displacement in order to avoid

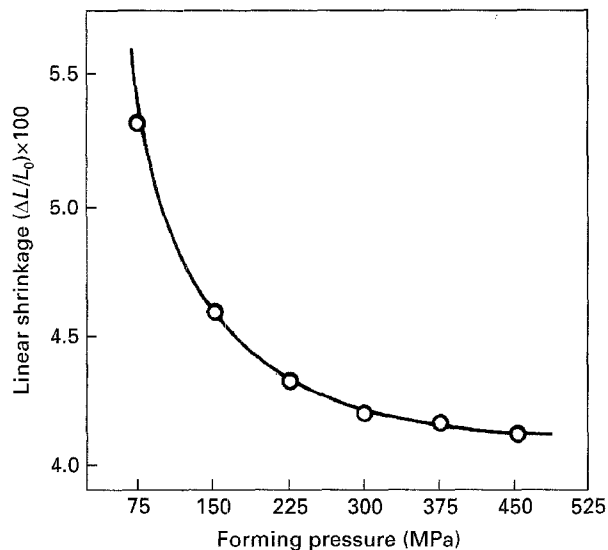


Figure 1 Effect of forming pressure ( $-45 \mu\text{m CaAl}_2\text{O}_4$  compacts).

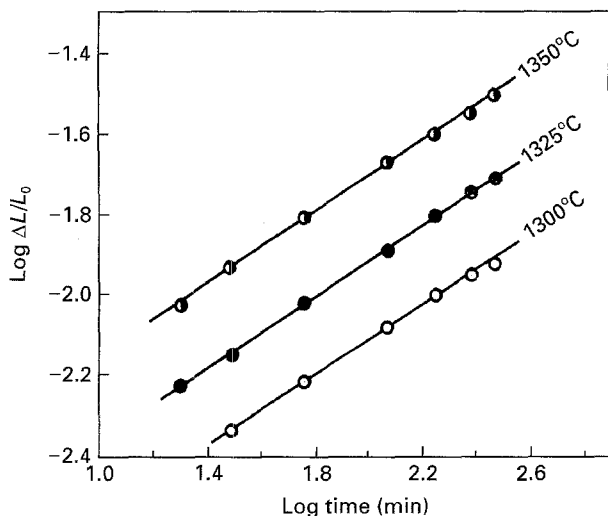


Figure 2 Logarithmic shrinkage plot of ( $-53 + 45 \mu\text{m CaAl}_2\text{O}_4$  compacts).

being misled by any anomalous shrinkage behaviour in a particular dimension. Linear shrinkage  $L/L_0$  was taken to be one third of the volume shrinkage  $V/V_0$ . The initial volume  $V_0$  was measured after prefiring the pellets at  $900^\circ\text{C}$  for 10 min. The initial dilation could not be correlated and hence it was ignored.

The time to reach the sintering temperature and the accompanying shrinkage can seriously affect the apparent shrinkage-time dependence [10]. The time error can be determined empirically as the correction that must be applied to the time of sintering of a given isotherm in order to straighten the log shrinkage versus log time curve. In the present study, the powder compacts were first preheated in the two zone silicon carbide furnace at  $900^\circ\text{C}$ , the temperature up to which the initial dilation was determined. The preheated pellets at  $900^\circ\text{C}$  were pushed into the sintering zone maintained at the sintering temperature and the actual sintering is assumed to begin 15 s after the pellets are introduced into the sintering chamber. The corrected initial hot length  $L_0$  and/or final hot length  $L$  of the

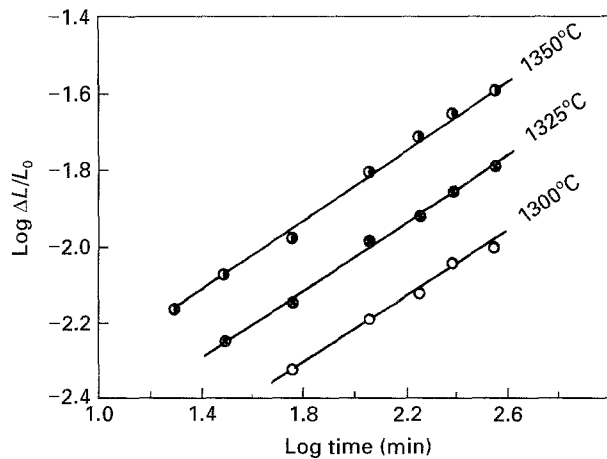


Figure 3 Logarithmic shrinkage plot of ( $-63 + 53 \mu\text{m CaAl}_2\text{O}_4$  compacts).

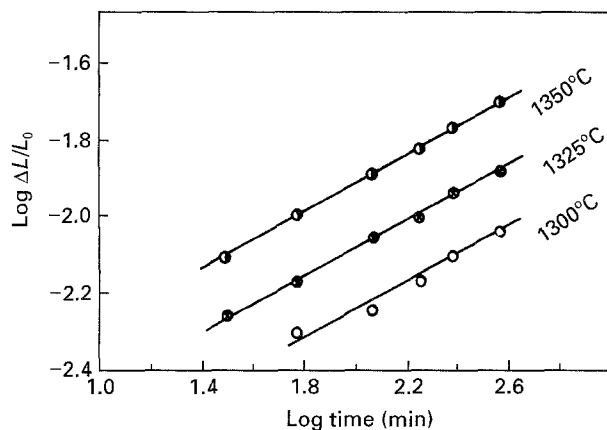


Figure 4 Logarithmic shrinkage plot of ( $-75 + 63 \mu\text{m CaAl}_2\text{O}_4$  compacts).

shrinkage compact is the cold length corrected for the thermal expansion of CA. Keeping in view the initial dilation and other factors, the initial and final volumes of the pellets were determined at room temperature by the displacement method. The effect of thermal expansion of  $\text{CaAl}_2\text{O}_4$  was assumed to be the same for both  $L_0$  and  $L$  values.

Figs 2-4 show linear plots obtained after applying suitable corrections for dilation and time. If the data for samples without the pre-firing at  $900^\circ\text{C}$  was plotted, there were some deviations especially at the beginning. It is apparent from Figs 2-4 that a change in the firing-time duration at different temperatures causes no significant change in the measured value of the gradient  $m$  in the chosen soaking period. The value of gradient  $m$  is  $\sim 0.40$  which means that the sintering rate is dependent on the temperature and also that the sintering is controlled by a volume diffusion mechanism of material transport [1, 2].

### 3.2. Temperature and particle size dependence

The true value of the sintering rate for  $-70 + 63$ ,  $-63 + 53$  and  $-53 + 45$  micron CA powder compacts has been determined by firing their compacts at

different temperatures. The method adopted involved firing a series of pellets for different times under identical conditions, at each of a series of temperatures. The data might be expected to exhibit a certain amount of scatter because of minor differences in behaviour amongst the pellets. However the prefiring performed to account for dilation and time corrections arising because of the initial behaviour of the pellets during heating to the sintering temperature should be able to fix the point for each of the pellets fired at a given temperature.

Compacts of the above three particle sizes were fired at 1300, 1325 and 1350°C for firing times between 10 and 360 min. It was found that by considering dilation and a small time correction for each of the plots a set of parallel lines with gradient  $m$  and acceptable linearity was obtained. Under these experimental conditions, no correction for initial shrinkage was necessary. The plots which passed through the average values of the shrinkage data are shown in Figs 2–4. Though the actual values of shrinkage for the three particle sizes at the three temperatures are different, the value of the gradient  $m$  was found to be  $\sim 0.40$  for all the lines, irrespective of temperature and particle size. It was possible to correlate the sintering time of one particle size with the other particle sizes which could give an equal shrinkage by considering a pair of particles (clusters) at a time by the following equation [11],

$$\Delta t_2 = \lambda^n \Delta t_1 \quad (4)$$

where  $t_1$  and  $t_2$  are the times necessary to accomplish a given fractional shrinkage or other proportional geometric change in the two respective particle sizes whose radii  $r_1$  and  $r_2$  are related by  $r_2 = \lambda r_1$ . The value of  $n$  is equal to 3 for the diffusion mechanism of material transport.

The sintering times necessary to produce a 3.0% volume shrinkage in  $-53 + 45$  micron powder compacts at 1350, 1325 and 1300°C are 20.0, 62.0 and 166.0 min whilst for  $-63 + 53$  and  $-75 + 63$  micron powder compacts the same shrinkage is obtained in 34.0, 107.0 and 286.0 and 54.0, 170.0 and 457.0 (extrapolated) min at the above mentioned temperatures respectively. If it is assumed that  $-53 + 45 \simeq 49$  microns,  $-63 + 53 \simeq 59$  microns and  $-75 + 63 \simeq 69$

microns so that  $\lambda_1 \simeq (-63 + 53)/(-53 + 45) \simeq 59/49 \simeq 1.2$ ,  $\lambda_2 = 69/49 \simeq 1.4$  and  $\lambda_3 = 69/59 \simeq 1.169$ ; and  $n = 3$  for volume diffusion; the values of  $\lambda_1^3 = 1.723$ ,  $\lambda_2^3 = 2.744$  and  $\lambda_3^3 = 1.5975$  are obtained. As  $\Delta t_1 = 20.0$  min at 1350°C for the  $-53 + 45$  micron powder compact to shrink by 3%,  $\Delta t_2$  for the  $-63 + 53$  micron compact at 1350°C to give the same shrinkage is equal to  $\lambda_1^3 \Delta t_1 = 1.723 \times 20 = 34.5$  min and  $\Delta t_3$  for the  $-75 + 63$  micron compact at same temperature is equal to  $\lambda_2^3 \times \Delta t_1 = 2.744 \times 20 = 54.8$  min, or  $\lambda_3^3 \times \Delta t_2 = 1.5975 \times 34.0 = 54.3$  min. The firing time required to produce a 3% shrinkage in the compacts, as obtained from the shrinkage plots are given in the top half of Table I and those obtained using Equation 4 are given in the bottom half. It can be seen that the calculated values of  $\Delta t$  are close to the values obtained by the shrinkage measurements where  $t$  is equal to the sintering time,  $t$  after applying necessary corrections.

It should be noted that Equations 1–4 are applicable if the initial particles used for the sintering are dense and single grains. Fig. 5a shows the grains of a twice fired  $\text{CaAl}_2\text{O}_4$  sample which showed an X-ray diffraction pattern identical to that expected from the literature (JCPDS: 23–1036) for CA. The lumps when reduced to  $-75 + 63$ ,  $-63 + 53$ ,  $-53 + 45$  and  $-45$  micron powders are expected to behave like dense grains, the true density of which was found to be  $2.98 \text{ g cm}^{-3}$  i.e., the theoretical density of  $\text{CaAl}_2\text{O}_4$ . Fig. 6 shows a plot of bulk density versus sintering time for  $-53 + 45$  micron powder compacts at 1350 and 1325°C. The bulk density of the compacts increased with the sintering time at each temperature. An increase in temperature was more effective than an increase in sintering time in increasing the bulk density. At 1350°C, a 240 min soaking produced a bulk density of  $2.3 \text{ g cm}^{-3}$ . There was no liquid phase formation (Fig. 5b) and thus the shrinkage was due to solid–solid sintering of  $\text{CaAl}_2\text{O}_4$  grains.

### 3.3. Evaluation of the activation energy

In Equation 3 the diffusion coefficient  $D = D_0 \exp(-Q/RT)$  where  $D_0$  is a pre-exponential constant and  $R$  is the gas constant. The activation energy can be obtained by plotting  $\log K'D$  as a function of

TABLE I Measured and calculated values of sintering time for 3.0% shrinkage at different temperatures for the three particle sizes

Temperature (°C)	Measured $t$ (min)			
	$-53 + 45 \mu\text{m}$ ( $\Delta t_1$ )	$-63 + 53 \mu\text{m}$ ( $\Delta t_2$ )	$-75 + 63 \mu\text{m}$ ( $\Delta t_3$ ) <sub>a</sub>	$-75 + 63 \mu\text{m}$ ( $\Delta t_3$ ) <sub>b</sub>
1350	20.0	34.0	53.7	
1325	63.0	107.0	169.8	
1300	166.0	286.0	457.0	
		Calculated $t$ (min)		
1350		34.5	54.8	54.3
1325		106.8	170.1	170.9
1300		286.0	455.5	456.8

$$\lambda_1 = 1.2, \lambda_2 = 1.4, \lambda_3 = 1.169$$

$$\Delta t_2 = \lambda_1^3 \Delta t_1, (\Delta t_3)_a = \lambda_2^3 \Delta t_1, (\Delta t_3)_b = \lambda_3^3 \Delta t_2$$

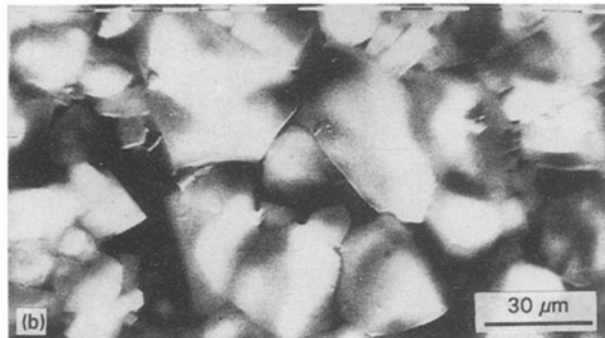
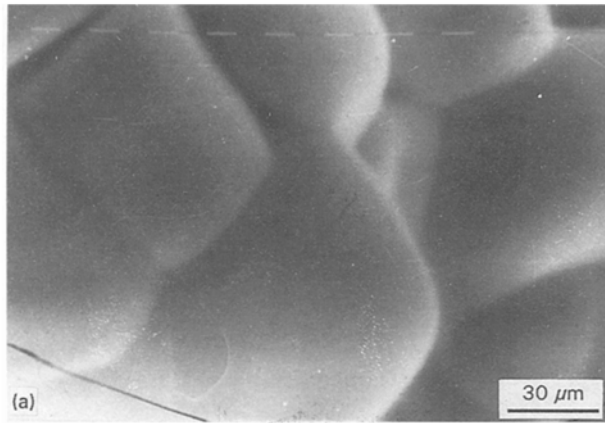


Figure 5 (a) SEM of  $\text{CaAl}_2\text{O}_4$  particles and (b) SEM of sintered  $\text{CaAl}_2\text{O}_4$  compacts fired at  $1350^\circ\text{C}$  for 2 h (fractured surface).

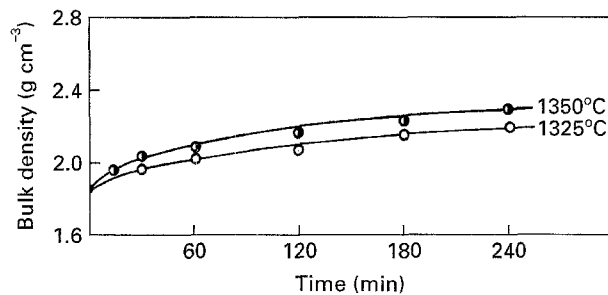


Figure 6 Densification of  $(-53 + 45)$   $\mu\text{m}$   $\text{CaAl}_2\text{O}_4$  compacts.

$1/T$ . In the present instance, the value of sintering time for a 3% shrinkage was determined at each temperature for the three particle sizes. The value of  $K'D$  was calculated using Equation 3 for the three particle sizes at different temperatures. It should be noted that the value of  $K'D$  is also influenced by the value of the power  $m$  and as the gradient  $m$  is nearly the same for the three particle sizes at different temperatures, it was considered fit for evaluating the value of the activation energy from the plots. The gradient of the plots (Fig. 7) for  $-75 + 63$ ,  $-63 + 53$  and  $-53 + 45$  was found to be the same which was equal to  $(0.5/0.125) \times 10^4$ . This gradient equals  $-Q/2.303R$  so that the activation energy for the sintering process is deduced as having the value  $Q = 2.303R \times 4 \times 10^4 = 183.04 \text{ Kcal mol}^{-1}$  ( $766.38 \text{ KJ mol}^{-1}$ ).

#### 4. Discussion

The calculation of the activation energy [12] in the present work involved two assumptions. The first is

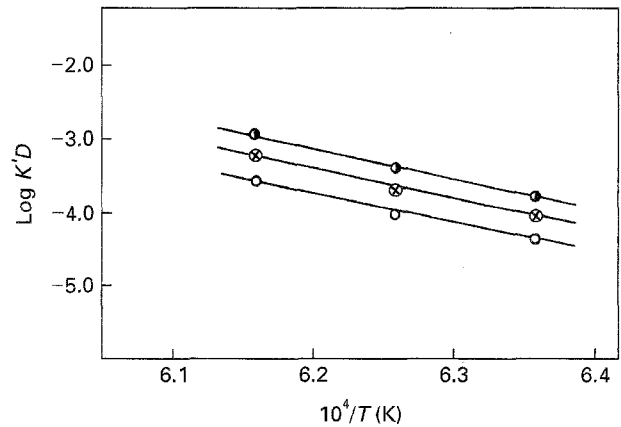


Figure 7 Arrhenius diagram for the sintering of  $\text{CaAl}_2\text{O}_4$ . The sintered compacts are: (●)  $-53 + 45 \mu\text{m}$ , (⊗)  $-63 + 53 \mu\text{m}$  and (○)  $-75 + 63 \mu\text{m}$ .

that the surface energy  $\gamma$  remains essentially constant with temperature. There is very little information in the literature about any variation of the surface energy with temperature. However it may be reasonable to expect it to be reduced by about one third on passing from room temperature to the melting temperature. This would cause the value of  $Q$  to be only about  $4.18 \text{ KJ mol}^{-1}$  lower than the calculated values [3]. The second assumption is for the average particle sizes in the different compacts, for example  $-53 + 45$ ,  $-63 + 53$  and  $-75 + 63$ . These particle sizes are close to the particle size of refractory cements of which  $\text{CaAl}_2\text{O}_4$  is a constituent. The rate of sintering or the gradient  $m$  is nearly 0.40 for all of the three particle sizes which means that a volume diffusion mechanism is operative in each case. Although  $Q$  may vary with the particle size [13] of the compact if the variation in the particle size is great, the activation energy calculated ( $766.38 \text{ KJ mol}^{-1}$ ) from the gradient of the Arrhenius plot in the present study is the same for the three particle sizes studied.

There was no phase separation or new phase formation (Fig. 5b) during the sintering process and these points were confirmed by the X-ray diffraction patterns of the  $\text{CaAl}_2\text{O}_4$  samples taken both before and after sintering. The X-ray diffraction pattern of calcium aluminate obtained by twice firing a 1:1 molar mixture of  $\text{CaO}$  and  $\text{Al}_2\text{O}_3$  was identical to the diffraction pattern obtained for sintered samples and showed the samples to be monocalcium aluminate. In the system  $\text{CaO}-\text{Al}_2\text{O}_3$ , only the  $\text{C}_{12}\text{A}_7$  phase is affected by  $\text{H}_2\text{O}$  at higher temperature [14]. It can absorb moisture at temperatures up to  $1350^\circ\text{C}$ . The other known stable calcium aluminates, e.g.  $\text{C}_3\text{A}$ ,  $\text{CA}$ ,  $\text{CA}_2$  &  $\text{CA}_6$  in this system are not affected by moisture at higher temperature. Thus at 1300, 1325 and  $1350^\circ\text{C}$  any effect of moisture on  $\text{CA}$  can be ignored. In addition there are no data available on any possible effect of  $\text{CO}_2$  on  $\text{CA}$  in the temperature range of the present study. The powders are dense grains and as shrinkage has taken place without any liquid phase, the volume diffusion mechanism is expected to operate.

The activation energy for the sintering of  $\text{CaAl}_2\text{O}_4$  is 5 times higher than the activation energy for its

formation [7] ( $152.3 \text{ KJ mol}^{-1}$ ) by the counter diffusion in a 1:1 CaO and  $\text{Al}_2\text{O}_3$  powder mix. The three species  $\text{Ca}^{2+}$ ,  $\text{Al}^{3+}$  and  $\text{O}^{2-}$  must diffuse for sintering to occur in  $\text{CaAl}_2\text{O}_4$  and the slowest diffusing species controls the sintering rate. The possibilities are the diffusion of  $\text{O}^{2-}$  ions or the calcium aluminate ( $\text{CaAl}_2\text{O}_4$ ) molecule, for which a high activation energy would be anticipated but to date there is insufficient data to enable this point to be clarified.

## 5. Conclusions

The initial stage sintering studies at various temperatures on  $\text{CaAl}_2\text{O}_4$  powders of  $-75 + 63$ ,  $-63 + 53$  and  $-53 + 45$  microns particle sizes are in accordance with a volume diffusion sintering mechanism with an activation energy of  $766.38 \text{ KJ mol}^{-1}$ . The sintering time of one particle size has been correlated with the other particle sizes which could give an equal shrinkage by considering a pair of particles at a time.

## References

1. W. D. KINGERY and M. BERG, *J. Appl. Phys.* **26** (1955) 1205.

2. D. L. JOHNSON and I. B. CUTLER, *J. Amer. Ceram. Soc.* **46** (1963) 545.
3. C. YINGJI and G. M. FRYER, *Trans. J. Br. Ceram. Soc.* **82** (1983) 170.
4. M. O. MARLOWE and K. R. WILDER, *J. Amer. Ceram. Soc.* **50** (1967) 509.
5. H. E. EXNER and G. PETZOW, in "Materials Science Research, Vol. 13, Sintering Processes", edited by G. C. Kuczynski, (Plenum, New York, 1980) pp. 107–120.
6. D. L. JOHNSON, *J. Appl. Phys.* **40** (1969) 192.
7. V. K. SINGH and M. M. ALI, *Trans. J. Br. Ceram. Soc.* **79** (1980) 112.
8. Powder Diffraction File, Card No. 23–1036, Joint Committee on Powder Diffraction Standards, Swarthmore, PA, 1973.
9. T. K. A. GHUDBBAN and G. M. FRYER, *Br. Ceram. Trans. J.* **84** (1985) 37.
10. K. W. LAY and R. E. CARTER, *J. Amer. Ceram. Soc.* **52** (1969) 189.
11. G. C. KUCZYNSKI, in "Sintering '85", edited by G. C. Kuczynski, D. P. Uskokovic, H. Palmour III and M. M. Ristic, (Plenum, New York, 1986) pp. 9–16.
12. T. WANG and R. RAJ, *J. Amer. Ceram. Soc.* **74** (1991) 1959.
13. V. K. SINGH and M. D. NARASIMHAN, *Trans. Ind. Ceram. Soc.* **34** (1975) 13.
14. V. K. SINGH and F. P. GLASSER, *Ceramic International* **14** (1988) 59.

*Received 13th June 1995*

*and accepted 18th March 1996*